Role of oxygen vacancies in the magnetic and dielectric properties of the high-dielectric-constant system $CaCu_3Ti_4O_{12}$: An electron-spin resonance study

M. A. Pires,* C. Israel, W. Iwamoto, R. R. Urbano, O. Agüero, I. Torriani, C. Rettori, and P. G. Pagliuso
Instituto de Física "Gleb Wataghin," UNICAMP, 13083-970, Campinas-SP, Brazil

L. Walmsley
Departamento de Física, Instituto de Geocincias e C. Exatas, Universidade Estadual Paulista, Rio Claro-SP, C.P. 178, CEP 13500-970, S.P., Brazil

Z. Le and J. L. Cohn
Physics Department, University of Miami, Coral Gables, Florida 33124, USA

S. B. Oseroff
San Diego State University, San Diego, California 92182, USA

(Received 4 October 2005; revised manuscript received 22 February 2006; published 2 June 2006)

We report experiments of electron spin resonance (ESR) of Cu^{2+} in polycrystalline samples of $CaCu_3Ti_4O_{12}$ post-annealed in different atmospheres. After being synthesized by solid state reaction, pellets of $CaCu_3Ti_4O_{12}$ were annealed for 24 h at 1000 °C under air, Ar or O_2. Our temperature dependent ESR data revealed for all samples nearly temperature independent g value (2.15(1)) and linewidth for $T \gg T_N \approx 25$ K. However, the values of ESR linewidth are strongly affected by the oxygen content in the sample. For instance, argon post-annealed samples show a much larger linewidth than the O_2 or air post-annealed samples. We attribute this broadening to an increase of the dipolar homogeneous broadening of the Cu^{2+} ESR lines due to the presence of oxygen vacancies which induce an $S=1/2$ spin inside the TiO_6 octahedra. Correlation between a systematic dependence of the ESR linewidth on the oxygen content and the high dielectric constant of these materials is addressed. Also, ESR, magnetic susceptibility, and specific heat data for a single crystal of $CaCu_3Ti_4O_{12}$ and for polycrystals of $CdCu_3Ti_4O_{12}$ are reported.

DOI: 10.1103/PhysRevB.73.224404 PACS number(s): 76.30.Fc, 77.22.-d, 75.50.Ee

I. INTRODUCTION

Recently, the body-centered perovskite-related compounds $ACu_3Ti_4O_{12}$ have attracted much attention due to the extremely high dielectric constant $\epsilon_0 \sim 10^4$ reported for ceramic and single crystals of the specimen with A=Ca.[1–3] High dielectric constant materials are very important for technological applications as in the case of capacitive memory devices. Aside from its potential technological application, the fundamental physics responsible for such enhanced dielectric constant has interested theorists and experimentalists working in this field. However, a definitive scenario to explain the large dielectric constant of $CaCu_3Ti_4O_{12}$ has not yet been established. Although a large ϵ_0 could have an intrinsic origin associated to Ca displacements, distortions of the TiO_6 octahedra, or small concentration of defects that disrupt the braced lattice, several reports have raised doubts about the intrinsic origin of such high value of ϵ_0.[4] For instance, Lunkenheimer *et al.* have proposed that the origin of the high value of the dielectric constant of $CaCu_3Ti_4O_{12}$ is simply an extrinsic effect associated with Maxwell-Wagner-type depletion layers at the sample contacts or at grain boundaries. On the other hand, subsequent studies[5] have shown that the addition of a buffer between the sample and the contacts has no influence on the large value of ϵ_0, indicating that the contacts alone cannot be responsible for these large values. Nevertheless, these studies relying on infrared measurements in $CaCu_3Ti_4O_{12}$ and $CdCu_3Ti_4O_{12}$ suggested that the giant measured dielectric constant of $CaCu_3Ti_4O_{12}$ is, at least in part, caused by an internal barrier layer capacitance (IBLC) effect.[5,6] This IBLC would be a consequence of the existence of semiconducting regions in the sample separated by insulating barriers.[5] However, this scenario, based on the IBLC effect, cannot fully explain the rapid suppression of ϵ_0 that occurs at low temperatures for $CaCu_3Ti_4O_{12}$, and also, the large decrease in the value of ϵ_0 caused by chemical substitution at the A=Ca site. Besides all the efforts trying to understand the origin of the giant dielectric constant, significant experimental work has been devoted to explore the evolution of the high dielectric constant of these materials as a function of chemical substitution (for example Ca-site and/or Ti-site doping) and sample preparation methods.[7–10] Although ϵ_0 has been found to strongly depend on these parameters, to establish a clear systematic correlation between a sample with certain characteristic (for instance, growth temperature and/or amount of doping) and its value of dielectric constant remains a challenge.

The magnetic susceptibility and electron spin resonance (ESR) experiments done in $CaCu_3Ti_4O_{12}$ are consistent with an antiferromagnetic ordering of the Cu^{2+} ions at $T_N=25$ K.[7,8,11] Above T_N, Raman scattering experiments have revealed short range magnetic fluctuations that increase with cooling following a T^{-1} dependence. The behavior of these fluctuations as a function of temperature was suggested to be related to the dramatic increase of ϵ_0 at high temperature.[1,11]

It is well established that for other oxides materials, variation in the oxygen stoichiometry gives rise to many complex and interesting behaviors. Examples are the colossal magneto-resistance manganites (CMR) and the high-T_C superconductor (HTSC) compounds.[12–15]

Here, we report measurements of ESR, magnetic susceptibility, specific heat, and dielectric constant in polycrystalline samples of $CaCu_3Ti_4O_{12}$ and $CdCu_3Ti_4O_{12}$ post-annealed in different atmospheres and in a $CaCu_3Ti_4O_{12}$ single-crystal grown in an image furnace. Our T-dependent ESR data show for all the samples, basically a T-independent g-value (2.15(1)) and linewidth for $T \gg T_N \approx 25$ K. But the values of the ESR linewidth and dielectric constant strongly depend on the oxygen content of the sample. Instead, the g value and the ordering temperature are unchanged by the annealing. Our results allowed us to conclude that the high value of the dielectric constant is dominated by an extrinsic IBLC effect. However, our data also indicated that there may be an intrinsic component of this large dielectric constant associated with the presence of oxygen vacancies, presumably in the TiO_6 octahedra, that disrupts the bracing in the lattice. Unfortunately, from our results we cannot separate these two contributions.

II. EXPERIMENT

Polycrystalline samples of $(Ca,Cd)Cu_3Ti_4O_{12}$ were grown by solid state reaction starting with $CaCO_3$ or CdO, CuO, and TiO_2. Stoichiometric powders of Ca base samples were heated at 900 °C for 12 h and then reheated at 1100 °C for 12 h more. A similar process was carried out for the Cd samples, but at 800 and 950 °C, for 12 h each, respectively. Finally, the samples were post-annealed for 24 h at 1000 °C for the Ca-based materials and at 900 °C for the Cd samples. A group of samples was reground after being heated for the first time and pelletized before the second heat treatment, and a second group was pelletized before the post-annealing. A last set of samples was not pelletized during the whole growth process (first, second, and post-annealing treatments) to allow for larger surface interchange. Some samples of this set were pelletized afterwards at room-T for specific measurements. The different sample growth treatments had the goal to obtain samples of different granularity (grain sizes and boundaries). The $CaCu_3Ti_4O_{12}$ single crystal was grown by a traveling-solvent floating zone method using an image furnace as described previously.[11] The $CaCu_3Ti_4O_{12}$ structure type and phase purity were confirmed by x-ray powder diffraction. For the studied samples, no measurable changes in the lattice parameters caused by annealing was observed. The presence of secondary phases were estimated to be less than 1%. The set of temperatures, heating, and annealing times were chosen to maintain sample integrity. A moderate departure from the listed annealing temperatures and times gave rise to a sample deterioration, mainly with a TiO_2 phase segregation. The ESR experiments were carried out in a conventional Bruker ESR spectrometer using a TE_{102} room-T cavity for X band and split-ring cavity for Q band. The sample temperature was varied using a helium gas-flux temperature controller. Specific heat measurements were performed in a Quantum Design PPMS small-mass calorimeter that employs a quasi-adiabatic thermal relaxation technique. Magnetization measurements were made in a Quantum Design dc superconducting quantum interference device and dielectric constant was extracted from impedance measurements performed with a Hewlett-Packard model 4263B LCR meter in the frequency range of 100 Hz–100 kHz. Silver paint electrodes, annealed at 300 °C, were applied on opposing edges of the specimens. Contact contributions to the impedance were eliminated for each specimen using measurements for several electrode separations.[18]

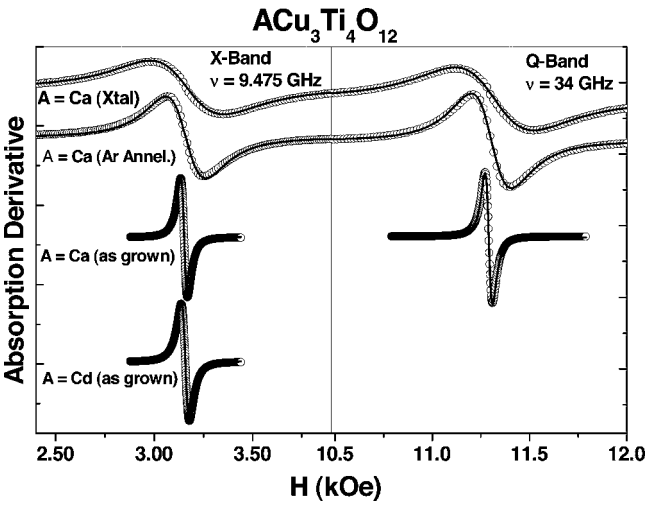

FIG. 1. Left-hand side: X-band ESR spectra for several samples $(Ca,Cd)Cu_3Ti_4O_{12}$. The solid lines represent fits to the spectra using single Lorentzian lines. Right-hand side: Q-band ESR spectra for selected samples of $CaCu_3Ti_4O_{12}$.

III. RESULTS

Figure 1 shows in the left-hand side the room-T X-band ($\nu \sim 9.5$ GHz) ESR spectra fitted to a single Lorentzian line for several samples of $(Ca,Cd)Cu_3Ti_4O_{12}$ as-grown and post-annealed under different conditions. This particular set of data belongs to powder samples that were not pelletized at all. The spectra show (for $T > 40$ K) a single resonance with a g value of 2.15(1) for all the samples. A large dependence on the atmosphere of the post-annealing treatment was found for the ESR linewidth for these samples. The broadest linewidths were observed for the polycrystalline argon annealed and the single crystals of $CaCu_3Ti_4O_{12}$. Although not studied in such detail, similar post-annealing linewidth behavior was observed for the $CdCu_3Ti_4O_{12}$ polycrystals (not shown). The Q-band ($\nu \sim 34$ GHz) spectra of the as-grown and argon post-annealed polycrystals, and the single crystals of $CaCu_3Ti_4O_{12}$ are shown on the right-hand side of Fig. 1. The g-value and the linewidth are frequency independent, i.e., the linewidths are not inhomogeneously broadened by a measurable g-value anisotropy and/or distribution. The ESR spectra intensity for all samples were compared to the intensity of a standard strong pitch with a known number of spins. From this analysis we found that for all samples the observed resonance comes from ~100% of the Cu^{2+} ions.

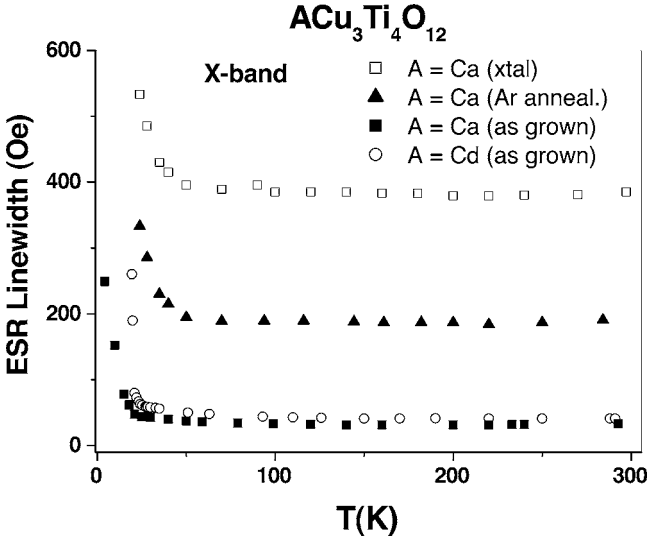

FIG. 2. Cu^{2+} ESR linewidth as a function of temperature for several samples of $CaCu_3Ti_4O_{12}$.

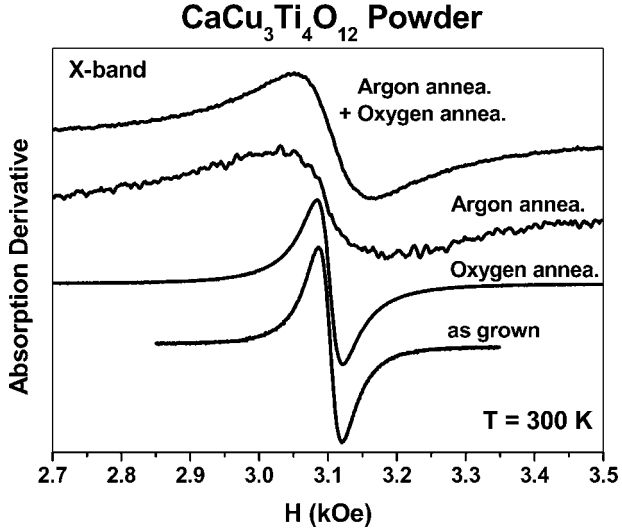

FIG. 3. *X*-band ESR spectra for several samples $CaCu_3Ti_4O_{12}$ after different post-annealing heat treatments.

The *T*-dependence of the ESR linewidth for the samples of Fig. 1 is shown in Fig. 2. For all samples, a nearly *T*-independent linewidth is observed for $T > 40$ K, with a small broadening at high-*T* (for $T \gtrsim 200$ K), as previously reported.[7,8] The weak *T*-dependence of the linewidth excludes the possibility of a Jahn-Teller distortion as being the origin of the dramatic increase of ϵ_0 observed above ~ 100 K.[11] Although the *T*-dependence of the ESR linewidth is similar for all samples, there is a *T*-independent contribution to the linewidth (ΔH_0) that strongly depends on the post-annealing atmosphere. For all temperatures (see Fig. 1), the argon post-annealed samples present broader linewidth than the air or oxygen annealed samples of $CaCu_3Ti_4O_{12}$. For the single crystal, the ESR linewidth is about one order of magnitude larger than that of the as-grown polycrystalline sample of $CaCu_3Ti_4O_{12}$.

Figure 3 shows the dramatic influence on the ESR spectra of the post-annealing treatment (air, Ar, or O_2) for the powder samples of $CaCu_3Ti_4O_{12}$ from the same set of samples of Figs. 1 and 2. While for samples annealed in air and O_2, the linewidth remains as narrow as for the as-grown samples $\Delta H \approx 40$ Oe, the argon annealed samples present a much broader ESR linewidth, $\Delta H \gtrsim 150$ Oe.

Thus, the Cu^{2+} ESR linewidth is strongly dependent on the oxygen content. We associate the line broadening with the presence of oxygen vacancies caused by the argon annealing. The broadening of the Cu^{2+} ESR linewidth for the argon post-annealed samples can be partially reverted when the same powder is re-annealed in O_2 (see Fig. 3). In contrast, the *g* value was found to be independent of the post-annealing treatments. It is important to point out that similar ESR linewidth behavior (Figs. 1–3) was observed for all groups of samples described in Sec. II. However when the post-annealing process was done on pellets of $CaCu_3Ti_4O_{12}$, the linewidth changes as function of the atmosphere were much less dramatic, presumably due to a smaller effective surface for O_2 exchange.

Magnetic susceptibility measured as a function of temperature at $H = 1$ kOe for an as-grown $CdCu_3Ti_4O_{12}$ sample and three samples of $CaCu_3Ti_4O_{12}$ (as-grown, single crystal, and argon-annealed) is shown in Fig. 4. For the polycrystalline samples, this particular set of data belongs to the group of samples that were pelletized at room-*T* only after the post-annealing treatment. However, as discussed in the following, the low-*T* magnetic susceptibility is only affected by the post-annealing treatment and not by the pelletizing process itself.

An antiferromagnetic phase transition is observed at $T_N = 25$ K for all the samples of $CaCu_3Ti_4O_{12}$ and at $T_N = 29$ K for the $CdCu_3Ti_4O_{12}$. At first glance, one can see the development of a low-*T* Curie tail for the argon post-annealed and the single crystal samples of $CaCu_3Ti_4O_{12}$. The *T*-dependence of the magnetic susceptibility of the as-grown and single crystalline sample of $CaCu_3Ti_4O_{12}$ is in excellent agreement with the data reported in Refs. 8 and 11, respec-

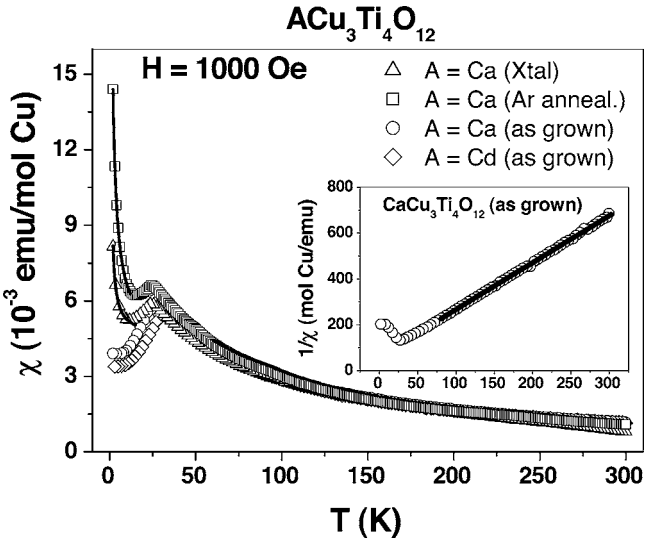

FIG. 4. Temperature dependence of the magnetic susceptibility taken with an applied field $H = 1$ kOe for select samples of $ACu_3Ti_4O_{12}$ (A=Ca and Cd) compounds.

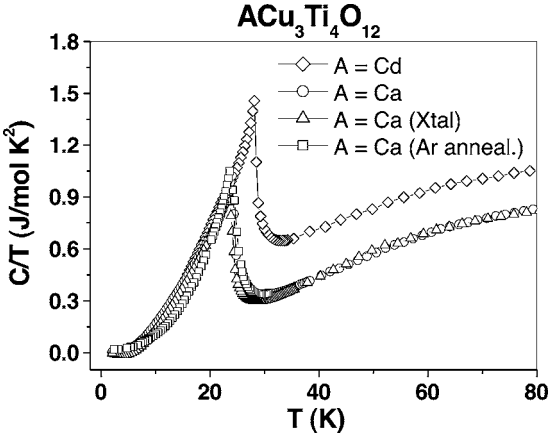

FIG. 5. Specific heat per mole divided by temperature as a function of temperature for select samples of $ACu_3Ti_4O_{12}$ (A =Ca and Cd).

tively. From the high-T Curie-Weiss linear fits of the inverse of the magnetic susceptibility, we have extracted the following Curie constants for the Ca-based samples, all given in (emu/(moleCu Oe K)): 4.70×10^{-1} (as grown), 4.48×10^{-1} (argon annealed), and 4.64×10^{-1} (single crystal). Assuming an Avogadro number of Cu^{2+} ions for the as-grown $CaCu_3Ti_4O_{12}$, we have obtained an effective magnetic moment of 1.94(4) Bohr magnetons for Cu^{2+} in the as-grown $CaCu_3Ti_4O_{12}$ and $CdCu_3Ti_4O_{12}$, and somewhat smaller Cu^{2+} effective moments for the argon annealed and single-crystal $CaCu_3Ti_4O_{12}$ samples. One may speculate that some Cu^{2+}, $S=1/2$, ions are missing in order to explain the decrease of the Curie constant for the argon annealed and single-crystal samples. One possibility is that the oxygen vacancies dope the material transforming some of the Cu^{2+} ions into nonmagnetic Cu^{1+} and some of the Ti^{4+} ions into magnetic Ti^{3+} with $S=1/2$. Support for such argument is given by the low-T Curie tail, observed for the argon annealed and single crystal samples, which may be attributed to Ti^{3+}. A Curie-Weiss fitting of the tail for those samples yields a Curie constant of 2.3×10^{-2} and 8.0×10^{-3} (emu/(moleTi Oe K)) for argon annealed and single crystal samples, respectively. Note that, for the argon annealed and single crystal samples of $CaCu_3Ti_4O_{12}$, the Curie constant, extracted from the high-T behavior plus that extracted from the Curie tail, is in good agreement with the Curie constant obtained for the as-grown $CaCu_3Ti_4O_{12}$. In other words, the number of Cu^{2+} ions summed to the number of Ti^{3+} ions for argon annealed and single crystal samples of $CaCu_3Ti_4O_{12}$ is similar to the number of Cu^{2+} ions in the as-grown $CaCu_3Ti_4O_{12}$ sample. From the fit to the low-T Curie tail, we estimated about 5% of non-interacting $S=1/2$ spins (oxygen vacancies) in the argon annealed and around 2% in the single crystal sample. The similarities between the data for the argon annealed polycrystals and the single crystal sample of $CaCu_3Ti_4O_{12}$ suggest that the $CaCu_3Ti_4O_{12}$ single crystals grown by a traveling-solvent floating zone method[11] are also oxygen deficient.

Figure 5 presents the low-T specific heat divided by T for the same set of samples of Fig. 4. Similar to the magnetic susceptibility data the macroscopic antiferromagnetic behavior remains unchanged by the post-annealing treatment. These results indicate that the macroscopic magnetic properties are not affected by the presence of oxygen vacancies. Furthermore the specific heat data are found to be the same for all groups of pelletized $CaCu_3Ti_4O_{12}$ samples described in Sec. II.

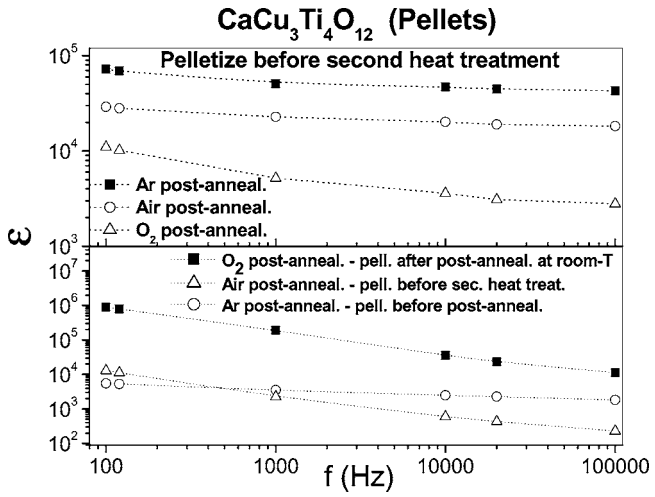

FIG. 6. Frequency dependence of the dielectric constant ϵ for several samples of $CaCu_3Ti_4O_{12}$ prepared and/or post-annealed in different conditions.

The frequency dependence of the dielectric constant ϵ_0 for several samples of $CaCu_3Ti_4O_{12}$ is presented in Fig. 6. The upper panel shows ϵ_0 for the post-annealed pellet samples of $CaCu_3Ti_4O_{12}$ belonging to the first group of samples described in Sec. II (pelletized before the second heat treatment). The lower panel displays ϵ_0 for selected post-annealed pellet samples subjected to the same temperature profile but pelletized in different stage of the heat treatment. This procedure was performed in order to create different compactness, granularity and/or grain sizes in the pellets [each sample belongs to a different group (Sec. II)]. It can be seen in the lower panel of Fig. 6, that when the pelletize process is performed at different stages of the sample growth, there is no correlation between the value of ϵ_0 and the post-annealing atmosphere. However, when the sample growth procedure is kept the same (upper panel, Fig. 6), higher ϵ_0 correlates with a higher oxygen vacancy concentration. Thus, as for the Cu^{2+} ESR linewidth, the value of ϵ_0 is larger for the argon annealed samples. These results suggest that when the large extrinsic contribution to the value of ϵ_0 is maintained roughly the same (presumably similar grain boundaries and IBLC effect) there seems to be a correlation between the value of ϵ_0 and the changes in the Cu^{2+} local environment, as probed by the ESR linewidth.

IV. DISCUSSION

Oxygen vacancies and/or intrinsic defects in oxides have been shown to play a crucial role in the physical properties of different classes of transition metal oxides such as HTSC, CMR, and ferroelectric compounds.[12–15] For the HTSC and CMR, among other effects, the variation in oxygen stoichi-

ometry strongly modifies the effective doping levels of the material which places the studied compound in different regions of its phase diagram.[14,15] In the latter compounds, oxygen vacancies are responsible for trapping electrons or inducing distortions/strain that can dramatically affect the dielectric properties of those materials.[12,13] When trapping electrons the oxygen vacancies defect can bind one or two electrons, giving rise to singly charged (F^+ centers) or to neutral F^0 center.[16,17]

As we discussed in the previous section, we found a large broadening of the Cu^{2+} ESR linewidth for samples with oxygen vacancies and in order to understand how this broadening can result from them, different contributions to the ESR linewidth must be considered.

There are two types of ESR line broadening in solids: homogeneous and inhomogeneous broadening. Homogeneous ESR linewidth is inversely proportional to the so-called *spin–spin* relaxation time, T_2.[19] It occurs when the magnetic resonance signal results from a transition between two levels of spins which are not sharply defined, but instead, are somewhat intrinsically broadened. The main contributions to homogeneous broadening are: (1) dipolar interaction between *like* spins, (2) spin-lattice interaction, (3) interaction with radiation field, (4) diffusion of excitation throughout the sample, and (5) motionally narrowing fluctuations of local fields.[19,20]

On the other hand, an inhomogeneously broadened resonant line is one which consists of a spectral distribution of individual lines merged into an overall line or envelope. For instance, a distribution of local fields caused by unresolved fine and/or hyperfine structure, g-value anisotropy, strain distribution and/or crystal irregularities that exceed the natural linewidth ($2/\gamma T_2$, γ is the gyromagnetic factor)[19,20] will make the spins in various parts of the sample feel different field strengths. In this way the resonance will be artificially broadened in an inhomogeneous manner. In the cases of inhomogeneous broadening caused by g-value anisotropy and related strain distribution and/or crystal irregularities, the ESR linewidths are expected to increase as a function of magnetic field. From Fig. 1 we see that the Cu^{2+} ESR linewidth for $ACu_3Ti_4O_{12}$ (A=Ca and Cd) is field (band-frequency) independent, therefore, we can rule out these contributions as the origin of the observed Cu^{2+} ESR linewidth.

For the homogeneous broadening, the spin-lattice interaction is the most important contribution to the ESR linewidths and it becomes dominant when the *spin-lattice* relaxation time, T_1, is comparable to T_2. In this case, the ESR linewidth is generally frequency independent but it is strongly temperature dependent (direct, Orbach, Raman, and exchange relaxation process) because it is ultimately coupled to the phonons. This behavior is in contrast to the nearly T-independent Cu^{2+} ESR linewidths observed for $T \gtrsim 40$ K in all our samples. Therefore, we conclude that *spin-lattice* relaxation cannot be the dominant mechanism responsible for the Cu^{2+} ESR linewidths in $ACu_3Ti_4O_{12}$ (A=Ca and Cd). Others sources for homogeneous broadening such as diffusion and motional narrowing process are unlikely to be present in our samples because the observed ESR lines arise from the Cu^{2+} ions that are fixed in the crystal lattice. Besides, there is no evidence for radiation field effects and the resonance line shapes are Lorentzian.

Therefore, the most probable homogeneous broadening mechanism present in our samples is the dipolar interaction between $S=1/2$ *like* spins. Van Vleck[21] has treated in detail the homogeneous line broadening mechanism involving dipolar and exchange interactions. For a simple cubic lattice of like spins a dipolar interaction produce a linewidth ΔH_{dd} given by[20–22]

$$\Delta H_{dd} = 2.3(g\beta\rho)[S(S+1)]^{1/2}, \tag{1}$$

where ρ is the density of spins/cm^3, g is the g value, and β is the Bohr magneton. When the exchange is very large compared to the dipolar energy, then the linewidth $\Delta H = \Delta\omega/\gamma$ is proportional to the square of the ΔH_{dd} divided by the rate of exchange[21,22]

$$\Delta H = \frac{1}{\gamma}\frac{(\Delta\omega_{dd})^2}{\omega_{\mathrm{ex}}}, \tag{2}$$

$$\Delta H = \frac{(\Delta H_{dd})^2}{H_{\mathrm{ex}}}, \tag{3}$$

and the exchange field $H_{\mathrm{ex}} = \omega_{\mathrm{ex}}\gamma$ is given by

$$H_{\mathrm{ex}} = (1.7J/g\beta\rho)[S(S+1)]^{1/2}, \tag{4}$$

where J is the exchange integral.

As long as the average distance between the Cu^{2+} spins remain unchanged, the dipolar and exchange interaction are T-independent, giving a line-broadening that is itself independent of temperature when $(g\beta H/kT) \ll 1$.[19] Therefore, the homogeneous broadening predicted by Eq. (3) would be consistent with the temperature and field independent Cu^{2+} ESR linewidth of Figs. 1 and 2 at high T. However, according to Eq. (3), either ΔH_{dd} should be increased and/or H_{ex} should be decreased by the vacancies in order to explain the enhanced line broadening observed for the argon post-annealed samples (see Figs. 2 and 3). Our results show that the antiferromagnetic transition at $T_N = 25$ K is not affected by the post-annealing process, thus we may infer that the exchange field H_{ex} is basically not modified by the level of vacancies present in our samples. Furthermore, in typical cases where the ESR linewidth is strongly narrowed by exchange interaction, the linewidth is expected to diminish at higher magnetic field as a consequence of the so-called 10/3 effect[19,20] and this was not observed in our ESR data. Therefore, the increasing of the linewidth for oxygen deficient samples is most likely associated to an increase of ΔH_{dd} due to the presence of the oxygen vacancies.

In the analysis of our magnetization curves (Fig. 4), we discussed that for the argon annealed and single crystal samples of $CaCu_3Ti_4O_{12}$ the data can be explained by the coexistence of antiferromagnetic coupled Cu^{2+} spins and a few percent of non-interacting $S=1/2$ spins. Equation (1) yields, for typical cubic paramagnetic salts with average distance between $S=1/2$ like spins of the order of 2–7 Å , to linewidths ranging from 50 to 500 Oe.[19,20] The Cu^{2+}-Cu^{2+} distance in cubic $CaCu_3Ti_4O_{12}$ is about 6 Å. Assuming that the loss of a oxygen atom would transform some of the Cu^{2+} ions into Cu^{1+} and, concomitantly, Ti^{4+} ions into Ti^{3+} ($S=1/2$ ions), the remaining majority of Cu^{2+} in the vicinity of

a TiO_6 octahedron would interact with a Ti^{3+} ($S=1/2$) at an average distance of roughly 3 Å. This new spin configuration would increase the effective homogenous dipolar interaction, however with contribution of dipolar interaction between the unlike Cu^{2+} and Ti^{3+} $S=1/2$ spins and could qualitatively explain the increase of ESR linewidth for the vacancy rich single crystal and argon-annealed sample of $CaCu_3Ti_4O_{12}$.

Therefore, based on our magnetization data and on the broadening of the Cu^{2+} we can conclude that oxygen vacancy defects in $CaCu_3Ti_4O_{12}$ are presumably F^+ centers. These centers may appear from a trapped electron at a $Ti^{3+}e_g(3d_{3z^2-r^2})$ orbital forming a paramagnetic complex.[16,17]

Now that we have qualitatively described a plausible scenario for the larger Cu^{2+} ESR linewidths in the oxygen deficient $CaCu_3Ti_4O_{12}$ samples, let us turn to the role played by the oxygen vacancies in the dielectric constants. In Fig. 6 we exemplified how the dielectric constant can be affected by the atmosphere of post-annealing process (upper panel) and by details of the sample preparation method (lower panel). The latter demonstrates how changes in the growth process can influence the value of the dielectric constants that are extrinsic in origin (e.g., associated with grain boundaries and IBLC effect[5,6]). However when the sample growth process is maintained the same and as controlled as possible, the dielectric constant is affected by the oxygen vacancies, as are the Cu^{2+} ESR linewidths.

Recently, others have studied the effects of post-annealing in thin films of $CaCu_3Ti_4O_{12}$ and they have found similar results to those reported here.[10] Also, careful studies using transmission electron microscopy have found that grain boundaries are oxygen vacancy richer than the grain interior.[23] Thus one may expect that the post-annealing process would create vacancies preferentially at the grain boundary, a fact also reflected in our samples. From the magnetic susceptibility low-T Curie tail (see Fig. 4) one can see that the argon post-annealed polycrystals present a higher number of vacancies than the $CaCu_3Ti_4O_{12}$ single crystal. However, the single crystals present a broader ESR linewidth than argon post-annealed samples. This result is easily explained by the fact that ESR linewidth arises from $\sim 100\%$ of the Cu^{2+} ions that are predominantly inside the grain. So Cu^{2+} ESR linewidth is more weakly broadened by vacancies present at the grain boundaries. In contrast, for the single crystals, all the vacancies are in the sample bulk, more effectively affecting the Cu^{2+} sites and giving rise to broader linewidths.

Regarding the effect of post-annealing process in ϵ_0 for these materials, based on the results mentioned above, one can argue that the effect seen in the upper panel of Fig. 6 is also an extrinsic effect caused by the enhancement of the IBLC affect due to the higher content of vacancies at the grain boundaries. We cannot rule out this scenario but we should point out that this explanation is not valid for the single crystals, and it is certainly bulk vacancy richer as measured by the ESR linewidth.

Also, for the polycrystalline samples, as the ESR linewidth reflects intrinsic properties from inside the grain, and it is not affected by pelletizing the powder on different stages of the growth, the apparent correlation seen in the upper panel of Fig. 6 between the oxygen vacancies, the Cu^{2+} ESR linewidths, and ϵ_0 opens the possibility of an intrinsic origin for at least part of the enhanced dielectric constant of these materials. As for the increase in the Cu^{2+} ESR linewidths for oxygen deficient samples, we discussed that oxygen vacancies may create an extra charge near the TiO_6 octahedra (tending to drive Ti^{4+} to Ti^{3+}). The presence of Ti^{3+} (or an extra charge) can disrupt the TiO_6 octahedra placing the Ti atoms in a slightly shifted position with respect to the oxygen cage and allowing for a local electrical polarization to appear.[11] Furthermore, paramagnetic complexes arising from Ti^{3+} ions coupled to an oxygen vacancy were experimentally found to occur in ferroelectric materials such as $BaTiO_3$.[13,16,17]

Therefore the presence of oxygen vacancies in the $CaCu_3Ti_4O_{12}$ and possible formation of Ti^{3+} could explain the broadening of Cu^{2+} ESR linewidths and shed some light on the origin of the large dielectric constants of $ACu_3Ti_4O_{12}$. Note that the IBLC and vacancy effects are difficult to separate from each other and in some cases are related. The combination of these effects may account for the conflicting data and interpretations in literature. A conclusive statement about the real intrinsic value ϵ_0 for $CaCu_3Ti_4O_{12}$ requires meticulous quantitative studies of oxygen vacancies, grains sizes, etc., for samples growing in well-controlled process, which is beyond the scope of this work. We concede that our interpretation regarding the role of oxygen vacancies in our ESR and magnetization data is somewhat speculative, and further TiO_6 and Cu-site local structure investigation (for instance done by Raman spectroscopy and x-ray absorption in carefully prepared post-annealed samples), would be valuable to confirm our interpretation.

Although studied less frequently, the Cd-based materials also show enhanced broadening of the ESR linewidth for post-argon annealed samples but the effect is smaller (10–20% broader linewidths for Ar-annealed. samples) than for $CaCu_3Ti_4O_{12}$. Larger values of ϵ_0, attributable to the IBLC effect, were also observed for the Cd samples, but the measured values of the Cd samples were always smaller (at least by a factor of 10) than for $CaCu_3Ti_4O_{12}$ prepared under the same condition. This result suggests that the Cd sample may be less susceptible to the creation of oxygen vacancies. Finally, we concluded that a single crystal of $CaCu_3Ti_4O_{12}$ prepared by a traveling-solvent floating zone method[11] behaves such as post argon-annealed polycrystals, suggesting that this crystal is oxygen deficient.

V. CONCLUSIONS

We report experiments of ESR of Cu^{2+} in polycrystalline samples of $ACu_3Ti_4O_{12}$ (post-annealed in different atmospheres) (A=Ca and Cd). From detailed studies in the Ca-based material we have shown that while the Cu^{2+} ESR g values and the ordering temperature are unaffected by the annealing, the ESR linewidths are dramatically changed by the oxygen content in the sample. Argon post-annealed samples show a much larger linewidth than the O_2 or air post-annealed samples. On the other hand, the dielectric constants for these materials were found to be affected by the

oxygen content in the sample as by the details on the sample preparation method. Our results agree with the growing evidence that most of the high value of the dielectric constant reported for $CaCu_3Ti_4O_{12}$ is due to an extrinsic effect of an internal barrier layer capacitance at grain boundaries but reveal the presence of oxygen vacancy induced Ti^{3+} centers in the bulk of these materials that may contribute to their intrinsic dielectric constant and manifest itself on other interesting physical properties of these materials.

ACKNOWLEDGMENTS

We thank J. L. Sarrao for helpful discussions. This work was supported by FAPESP (SP-Brazil) Grant Nos. 04/08798-2, 03/09861-7, 00/08649-6, CNPq (Brazil) Grant. Nos. 307668/03 and 04/08798-2 and 304466/20003-4 and NSF (USA) DMR 0102235. Research at the University of Miami was supported by the NSF under Grant DMR-0072276 and by an award from Research Corporation.

*Permanent address: Universidade Federal de Gois, 74001-970 Goinia-Go, Brazil.

[1] M. A. Subramanian, D. Li, N. Duan, B. Reisner, and A. W. Sleight, J. Solid State Chem. **151**, 323 (2000).
[2] A. P. Ramirez, M. A. Subramanian, M. Gardel, G. Blumberg, D. Li, T. Vogt, and S. M. Shapiro, Solid State Commun. **151**, 217 (2000).
[3] C. C. Homes, T. Vogt, S. M. Shapiro, S. Wakimoto, and A. P. Ramirez, Science **293**, 673 (2001).
[4] P. Lunkenheimer, V. Bobnar, A. V. Pronin, A. I. Ritus, A. A. Volkov, and A. Loidl, Phys. Rev. B **66**, 052105 (2002).
[5] C. C. Homes, T. Vogt, S. M. Shapiro, S. Wakimoto, M. A. Subramanian, and A. P. Ramirez, Phys. Rev. B **67**, 092106 (2003).
[6] D. C. Sinclair, T. B. Admas, F. D. Morrison, and A. R. West, Appl. Phys. Lett. **80**, 2153 (2002).
[7] E. Giulloto, M. C. Mozzati, C. B. Azzoni, V. Massarotti, and M. Bini, Ferroelectrics **298**, 61 (2004).
[8] M. C. Mozzati, C. B. Azzoni, D. Capsoni, M. Bini, and V. Massarotti, J. Phys.: Condens. Matter **15**, 7365 (2003).
[9] M. A. Subramanian and A. W. Sleight, Solid State Sci. **4**, 347 (2002).
[10] L. Fang, M. Shen, and W. Cao, J. Appl. Phys. **95**, 6483 (2004).
[11] A. Koitzsch, G. Blumberg, A. Gozar, B. Dennis, A. P. Ramirez, S. Trebst, and S. Wakimoto, Phys. Rev. B **65**, 052406 (2002).
[12] A. J. Bosman and H. J. van Daal, Adv. Phys. **19**, 1 (1970).
[13] S. Lenjer, O. F. Schirmer, H. Hesse, and Th. W. Kool, Phys. Rev. B **66**, 165106 (2002).
[14] J. G. Bednorz and K. A. Mller, Rev. Mod. Phys. **60**, 585 (1988).
[15] M. B. Salamon and M. Jaime, Rev. Mod. Phys. **73**, 583 (2001).
[16] R. Scharfschwerdt, A. Mazur, O. F. Schirmer, H. Hesse, and S. Mendricks, Phys. Rev. B **54**, 15284 (1996).
[17] V. V. Laguta, A. M. Slipenyuk, I. P. Bykov, M. D. Glinchuck, M. Maglione, D. Michau, J. Rosa, and L. Jastrabik, Appl. Phys. Lett. **87**, 022903 (2005).
[18] J. L. Cohn, M. Peterca, and J. J. Neumeier, J. Appl. Phys. **97**, 034102 (2005).
[19] A. Abragam and B. Bleaney, *Electron Paramagnetic Resonance of Transition Ions* (Clarendon, Oxford, 1670).
[20] C. P. Poole and H. A. Farach, *Relaxation in Magnetic Resonance* (Academic, New York, 1971).
[21] J. H. Van Vleck, Phys. Rev. **74**, 1168 (1948).
[22] P. W. Anderson and P. R. Weiss, Rev. Mod. Phys. **25**, 269 (1953).
[23] L. Wu, Y. Zhu, S. Park, S. Shapiro, G. Shirane, and J. Tafto, Rev. Mod. Phys. **25**, 269 (1953).